Crack Growth Under Long-Term Static Loads: Characterizing Creep Crack Growth Behavior in Hydrogenated Nitrile

W. V. Mars
Endurica LLC, Findlay, Ohio, USA

K. Miller
Axel Products, Inc., Ann Arbor, Michigan, USA

S. Ba & A. Kolyshkin
Schlumberger, Houston, Texas, USA

ABSTRACT: When a load is carried over an extended period, a crack in a viscoelastic material might grow, even if the load is less than the static tearing strength T_c for unstable rupture, and even in the absence of dynamic cycles. The rate of crack growth under these conditions is governed by the instantaneous value of the energy release rate. In the oil and gas industry, a seal or packer may well be required to tolerate high pressures encountered for an extended time without developing a crack in the material, even in the absence of dynamic cyclic loading. In this case, understanding the development of time-dependent cracking is essential to the successful material selection and design. A finitely scoped, strain-controlled procedure was used in which static strain is slowly increased on a planar tension test piece over a prespecified total test duration while a camera records images of crack development. The procedure was applied on a carbon black-filled hydrogenated nitrile. The information obtained in the experiment can be used to evaluate creep-crack growth, or in combination with measurements of the fatigue crack growth rate law, to analyze cases where crack growth might occur under mixed conditions.

Crack growth sometimes occurs under loads less than those required to produce an unstable rupture. In dynamic applications, for example, cyclic loads can induce significant crack growth (Thomas 1958; Gent & Mars 2012). In static applications, given sufficient time, crack growth might also occur due to a creep mechanism (Greensmith & Thomas 1955; Lake & Lindley 1964a, Kadir & Thomas 1981, Bhowmick 1986).

There are many applications involving long-term, subcritical static loading that exceeds the intrinsic strength. The intrinsic strength represents conditions under which an elastomer may be expected to operate indefinitely without crack growth. The project being presented in this paper was motivated by the need to characterize creep-crack growth rate behavior for high-pressure, high-temperature (HPHT) applications in the energy industry (Zhong 2016, Mody et al 2013, Shell 1980). Thermoplastic elastomers are another application where creep effects are sometimes significant (Mars and Ellul 2017).

The characterization of creep-crack growth is founded upon the energetic framework of Rivlin and Thomas (1953). In their framework, crack tip conditions are parameterized by means of the energy release rate T, which relates prospective changes in the total stored energy U to prospective changes in the projected surface area A of a given crack, given by the following equation:

$$T = -\frac{dU}{dA} \tag{1}$$

Equation (1) represents the energy released during fracture per unit of newly created fracture surface area. The energy release rate has been applied extensively to strength and fatigue problems (Rivlin & Thomas 1953, Gent & Mars 2012, Mars 2007), where its ability to objectively relate results across a wide range of test pieces and crack configurations has no rival.

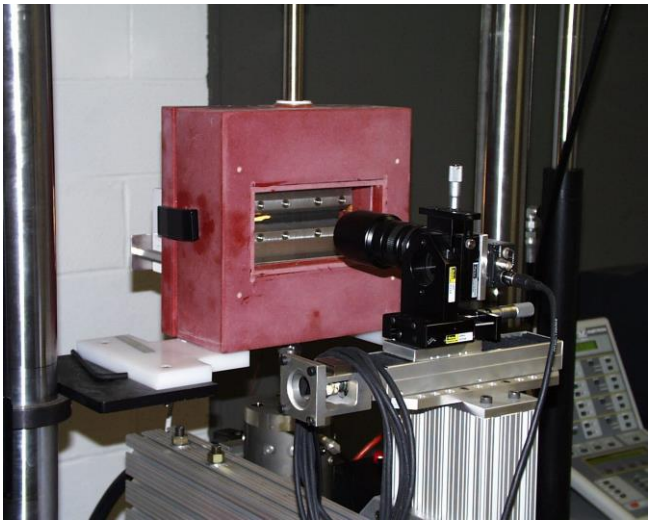

Figure 1. Testing system with environmental chamber, back-lit planar tension specimen, and camera.

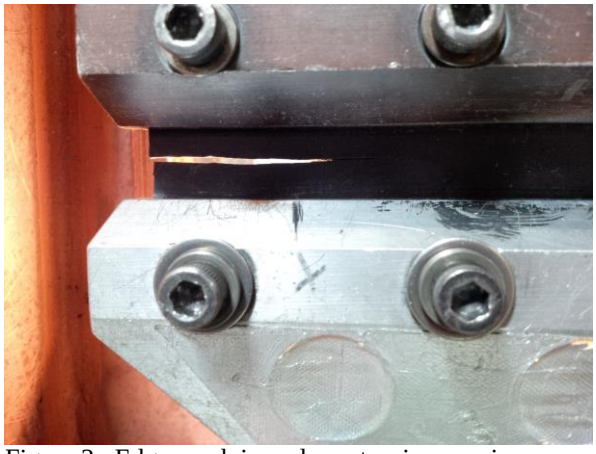

Figure 2. Edge crack in a planar tension specimen.

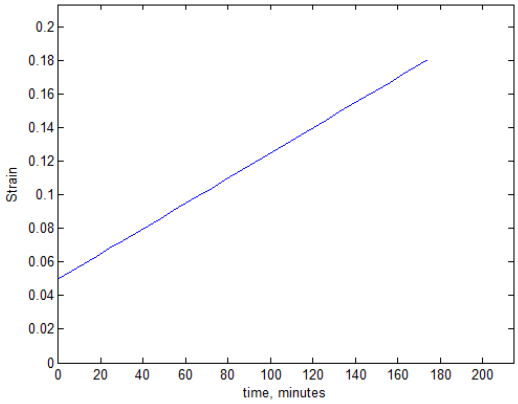

Figure 3. Strain ramp used to drive creep crack growth.

Subject to certain limitations, this energy release rate might also be applied to comprehending static applications involving creep, particularly when the creep process is predominantly localized at the crack tip (Netzker et al. 2013), as it often will be in problems involving the development of small cracks (Aït-Bachir et al. 2012). The work presented in this paper applies an experimental procedure using the system shown in Figure 1 for observing creep-crack growth, and to derive the characteristic creep-crack growth rate curve.

In general, the total rate of crack growth is the sum of the cycle-dependent and time-dependent components according to Lake & Lindley (1964a) and Busfield et al. (2002), and as given by:

$$\frac{dc}{dN} = \frac{\partial c}{\partial N} + \frac{\partial c}{\partial t}\frac{dt}{dN} \tag{2}$$

Here, c = crack length
t = time and
N = number of applied cycles.

The first term is the cyclic fatigue crack growth rate, which is a function of the peak energy release rate T_{max}, and the ratio $R = T_{min} / T_{max}$. T_{min} is the minimum energy release rate of the applied cycle, given by the following:

$$\frac{\partial c}{\partial N} = f(T_{max}, R) \tag{3}$$

The factor $\partial c/\partial t$ in the second term is the creep-crack growth rate. This growth rate depends on the instantaneous energy release rate $T(t)$, and is important in non-crystallizing rubbers. It follows this rule:

$$\frac{\partial c}{\partial t} = g(T(t)) \tag{4}$$

The factor dt/dN in the second term of equation (2) is the time duration of each cycle.

Commercial fatigue codes like fe-safe/Rubber™ and Endurica CL™ enable the user to independently specify equations (3) and (4), so that they may be considered in the critical plane analysis (Barbash and Mars 2016) of elastomer part durability. The purpose of the work being presented in this paper is to measure the creep component of the relationship $g(T)$.

1 EXPERIMENTAL

The material being tested in this work is a proprietary filled, hydrogenated nitrile (HNBR) compound used in the oil and gas industry.

The experiment used a single-edge-cut planar tension specimen (see Figure 2). After cutting the specimen with a razor, the specimen was loaded under a slowly and linearly increasing strain during the test period. As the strain increased, the crack length was imaged continuously. Simultaneously, measurements of the load and displacement were collected, enabling calculation of the energy release rate on the crack at any given time during the test.

The dimensions of the planar tension specimen were 150 mm x 10 mm x 2 mm. The width was large relative to the height so that homogeneous straining was assumed (Castellucci et al. 2008). The initial cut, made via razor blade to a depth of 25 mm, was at least 2.5 times larger than the gauge height of the specimen to avoid undesired edge effects.

From prior measurements made on this material, it was known that the intrinsic strength (Lake & Thomas 1967, Lake & Yeoh 1980, Bhowmick 1983, Mars et al 2016) is T_0 = 93 J/m^2, and that the critical tearing energy at unstable rupture is T_c= 5030 J/m^2.

1.1 *Control*

The strain ε applied to the specimen was initially 5%, and was increased linearly at a rate of 4.5%/hour until the test was completed (see Figure 3). The testing system features a temperature chamber. In the present work, the chamber temperature was maintained at 100°C.

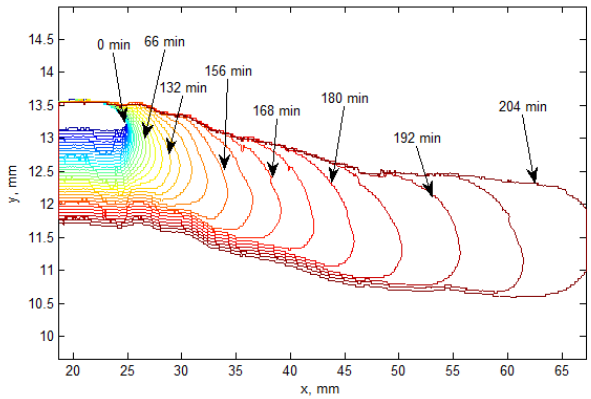

Figure 4. Crack images recorded and overlaid to show the crack tip progression during the experiment. Note that the y- axis is exaggerated relative to the x- axis.

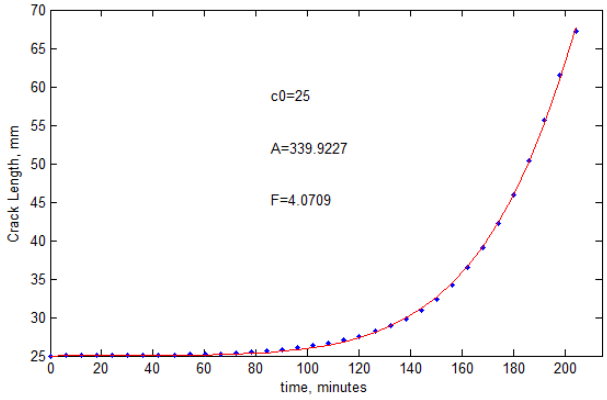

Figure 5. Crack length history, observed (dots) and fitted (solid line).

1.2 *Measurement*

Strain in the specimen was determined by dividing the crosshead displacement by the gauge height h. The engineering stress σ was determined from the force recorded by a 4-kN load cell. The non-cracked cross-sectional area was computed based on the unstressed specimen dimensions, and taking into account the instantaneous length of the developing crack, which was recorded with a camera. One can spot the camera position in front of the specimen in Figure 1. Figure 4 shows typical images taken by the camera with the time each picture was taken recorded.

The strain energy density W is estimated by integrating the stress-strain curve. This integration can be done numerically by computing the area in between the stress-strain curve.

$$W = \int \sigma d\varepsilon \tag{5}$$

2 RESULTS AND ANALYSIS

The energy release rate, T, at each instant was computed using equation (6), where h, the specimen gauge height, was 10 mm.

$$T = Wh \tag{6}$$

If it is assumed that the creep-crack growth rate law follows a power law relation between the energy release rate and the crack growth rate, it then follows that the length history $c(t)$, for a given history of strain energy density W, is given by:

$$c = c_0 + r_q \left(\frac{h}{T_q}\right)^F \int_0^t W^{F_q} dt = c_0 + A \int_0^t W^{F_q} dt \tag{7}$$

where c = the crack length, mm

c_0 = the initial crack length, prior to application of any cycles, mm

t = time, s

A is a parameter derived from the curve fitting process that reflects the combined influence of the material parameters r_c, T_c, and F, and the specimen gauge height h.

Crack images collected during the experiment were digitized and plotted as shown in Figure 4. In this figure, the colors represent time, with blue indicating early times and red corresponding to late times. From this information, the crack length history can be derived. Figure 5 shows typical crack length vs. time history, and the curve fit of equation (7) to the observations.

An error sum E was minimized to obtain the fit parameters c_0, A, and F_q. The integral was evaluated numerically during minimization to reflect the actual observed history $W(t)$ as follows:

$$E = \left(c(t) - \left[c_0 + A \int W^{F_q} dt\right]\right)^2 \tag{8}$$

Crack growth rates dc/dt were determined by differentiating equation (7) with respect to time at each of the times for which crack length and stress/strain were recorded by the testing system. The crack growth rate was then plotted as a function of the energy release rate T, as shown in Figure 6. The following power law was then fit to the results:

$$\frac{dc}{dt} = BT^{F_q} = r_q \left(\frac{T}{T_q}\right)^{F_q}. \tag{9}$$

Due to the differentiation, it might be a challenge to have robust numerical fitting of the data. It has been found that using the method above for determining the slop F_q allows to have good precision on the value from about three replicates only. This is a great advantage as it reduces the testing time required to get good estimate of the slope.

To avoid the strange units on fit parameter B, the parameters r_q and T_q are chosen to normalize the results relative to the uppermost point of the curve.

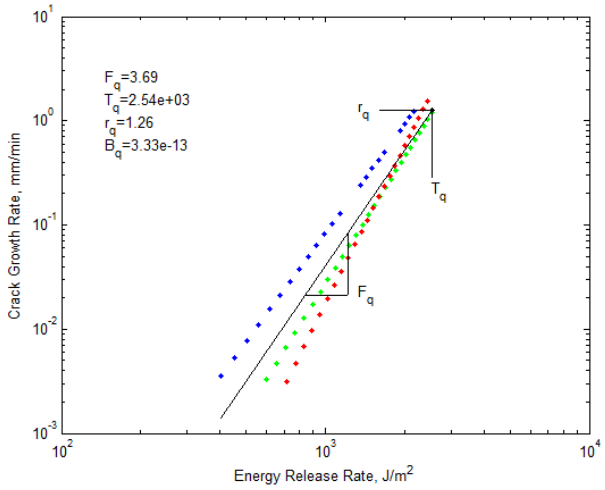

Figure 6. Creep-crack growth rate curves (3 replicates).

Table 1. Fitted power law creep crack growth parameters. (mm/min vs. J/m^2)

Material	HNBR
Fq	3.69
Tq, kJ/m^2	2.54
rq, mm/min	1.26

3 DISCUSSION

It is interesting to compare the fatigue (cyclic) crack growth with the creep crack growth per cycle. For computing the creep crack growth per cycle, one needs to integrate it over one cycle similar to what was done by Busfield et al. (2002). For example, the incremental crack length can be expressed as:

$$\Delta c = \int_0^{t_0} B_q (T(t))^{F_q} \, dt \qquad (10)$$

Where t_0 represents the time period of one fatigue cycle.

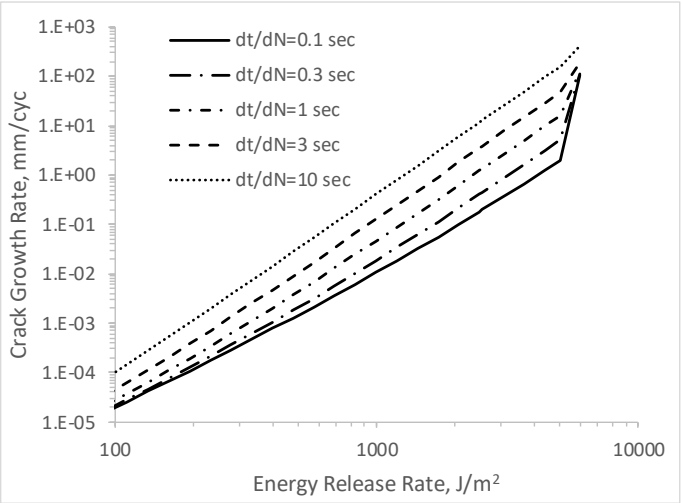

Figure 7. Total cyclic crack growth rate for a series of different cycle periods, computed via equation (2).

For the subject material, the fatigue crack growth rate law exhibited a powerlaw slope of F0=2.55, a critical tearing energy Tc = 3.05 kJ/m2, and rc=0.40 mm/cyc. Figure 7 plots combined creep-fatigue rate curves, via equation (2), for a series of different values of the cycle period dt/dN ranging from 0.1 seconds to 10 seconds. Longer times are seen to produce larger per-cycle rates, due to the creep effect, as expected. Shorter times are seen to eliminate the creep effect, with the rate curve approaching the cyclic fatigue crack growth rate curve.

Also, the slop F_q =3.69 is higher than the value F_c =2.55 obtained for the same material in pure fatigue crack growth test. The steeper slope of the creep crack growth rate law seems to suggest that the crack tip dissipation occurring during the creep process is perhaps weaker than that occurring during the cyclic process, since low slope is known to be associated with the strength of crack tip dissipation processes (Lake and Thomas 1967).

Note also that this result implies that at long times (or low frequency), and at high loads, it becomes increasingly important to characterize both fatigue and creep crack growth contributions, and to use the full form of equation (2) to estimate the service life.

4 CONCLUSION

An experimental procedure for observing the time-dependent creep-crack growth rate law has been implemented. The measurement is useful when designing for loads that must be supported over a long period, and when analyzing fatigue performance under conditions involving mixed cyclic and time-dependent crack growth. The slope of the creep-crack growth rate law is not necessarily the same as the slope of the fatigue crack growth rate law. Indeed, in the case of filled HNBR, the creep slope was significantly higher than the fatigue slope.

REFERENCES

Aït-Bachir, M., Mars, W. V., Verron E, 2012. "Energy release rate of small cracks in hyperelastic materials." *International Journal of Non-Linear Mechanics* 47, no. 4: 22-29.

Barbash, K. P., & Mars, W. V. (2016). Critical Plane Analysis of Rubber Bushing Durability under Road Loads (No. 2016-01-0393). SAE Technical Paper.

Bhowmick, A. K., A. N. Gent, and C. T. R. Pulford. 1983. "Tear strength of elastomers under threshold conditions." *Rubber Chemistry and Technology* 56, no. 1: 226-232.

Bhowmick, A. K. 1986. Tear strength of elastomers over a range of rates, temperatures, and crosslinking: tearing energy spectra. *Journal of Materials Science*, 21(11), 3927-3932.

Busfield, J. J. C., K. Tsunoda, C. K. L. Davies, and A. G. Thomas. 2002. "Contributions of time dependent and cyclic crack growth to the crack growth behavior of non-strain-crystallizing elastomers." *Rubber Chemistry and Technology* 75, no. 4: 643-656.

Castellucci, M. A., A. T. Hughes, and W. V. Mars. 2008. "Comparison of test specimens for characterizing the dynamic properties of rubber." *Experimental Mechanics* 48, no. 1: 1-8.

Gent, A. N., and W. V. Mars. 2012. "Strength of elastomers." *Science and Technology of Rubber*: 419-454.

Greensmith, H. W., and A. G. Thomas. 1955. "Rupture of rubber. III. Determination of tear properties." *Journal of Polymer Science* 18, no. 88: 189-200.

Kadir, A., & Thomas, A. G. 1981. Tear behavior of rubbers over a wide range of rates. *Rubber Chemistry and Technology*, 54(1), 15-23.

Lake, G. J. Lindley P. B., 1964a. "Cut Growth and Fatigue of Rubbers. II. Experiments on a Noncrystallizing Rubber", *Journal of Applied Polymer Science*, Vol. 8, pp. 455-466.

Lake G.J., Lindley P.B., 1964b. Ozone Cracking, flex cracking and fatigue of rubber, *Rubber Journal*, Vol 146, No. 11, pp. 30-39, 1964b.

Lake, G. J., and A. G. Thomas. 1967. "The strength of highly elastic materials." *Proceedings of the Royal Society of London A: Mathematical, Physical and Engineering Sciences*, vol. 300, no. 1460, pp. 108-119. The Royal Society.

Lake, G. J., and O. H. Yeoh. 1980. "Measurement of rubber cutting resistance in the absence of friction." *Rubber Chemistry and Technology* 53, no. 1: 210-227.

Mars W. V., R. Stocek, C. Kipscholl, October 10-13, 2016, Intrinsic Strength Analyzer Based on the Cutting Method, Paper #79, Fall 190th Technical Meeting of the Rubber Division of the American Chemical Society, Inc., Pittsburgh, PA, ISSN: 1547-1977.

Mars, W. V. 2007. "Fatigue life prediction for elastomeric structures." *Rubber Chemistry and Technology* 80, no. 3: 481-503.

Mars, WV, Ellul MD, 2017. Fatigue Characterization of a Thermoplastic Elastomer, *Rubber Chemistry and Technology*, 90, no. 2.

Mody, R., D. Gerrard, and J. Goodson. 2013. "Elastomers in the Oil Field." *Rubber Chemistry and Technology* 86, no. 3: 449-469.

Netzker, C., T. Horst, K. Reincke, R. Behnke, M. Kaliske, G. Heinrich, W. Grellmann. 2013. "Analysis of stable crack propagation in filled rubber based on a global energy balance." *International Journal of Fracture* 181, no. 1: 13-23.

Rivlin, R. S., and A. G. Thomas. 1953. "Rupture of rubber. I. Characteristic energy for tearing." *Journal of Polymer Science* 10, no. 3: 291-318.

Shell, Robert L. 1980. "Test for Evaluating Extrusion Resistance for Oil Well Packer Applications." *Rubber Chemistry and Technology* 53, no. 5: 1239-1260.

Thomas, A. G. 1958. "Rupture of rubber. V. Cut growth in natural rubber vulcanizates." *Journal of Polymer Science* 31, no. 123: 467-480.

Zhong, Allan. 2016. "Challenges for High-Pressure High-Temperature Applications of Rubber Materials in the Oil and Gas Industry." In Residual Stress, Thermomechanics & Infrared Imaging, *Hybrid Techniques and Inverse Problems*, Volume 9, pp. 65-79. Springer International Publishing.